

# Comparison of Mechanical Properties of Trabecular Bone Derived from $\mu$ MRI and $\mu$ CT

C. S. Rajapakse<sup>1</sup>, J. Magland<sup>1</sup>, S. L. Wehrli<sup>2</sup>, X. H. Zhang<sup>3</sup>, X. S. Liu<sup>3</sup>, X. E. Guo<sup>3</sup>, and F. W. Wehrli<sup>1</sup>

<sup>1</sup>Laboratory for Structural NMR Imaging, Department of Radiology, University of Pennsylvania School of Medicine, Philadelphia, Pennsylvania, United States, <sup>2</sup>Children's Hospital of Philadelphia, Philadelphia, Pennsylvania, <sup>3</sup>Department of Biomedical Engineering, Columbia University, New York, New York, United States

**Introduction** Prediction of fracture risk is of prime importance for the assessment of the effectiveness of therapeutic intervention of patients with osteoporosis. Currently, bone densitometry is used for this purpose. However, studies have shown that prediction of bone strength can be greatly improved by including the bone's structural properties in the analysis [1, 2]. Recent advances in *in-vivo*  $\mu$ MRI now allow noninvasive assessment of TB architecture [3]. The aim of this work was to address to what extent mechanical properties of trabecular bone (TB) -- Young's and shear moduli -- derived from  $\mu$ MR images, compare with those obtained by high resolution  $\mu$ CT. To answer this question ten TB samples were imaged using  $\mu$ MR and  $\mu$ CT and mechanical constants derived from these two data sets, using micro finite-element ( $\mu$ FE) analysis, were compared with each other.

**Methods** Ten TB samples (five femur, three lumbar and three tibia) were cored using Core Drills 102057 (Starlite Industries, Inc.) with inner diameter 5.20mm and imaged with by  $\mu$ CT (Scanco Medical VivaCT 40) and 400 MHz MRI (Bruker DMX 400) at 21 $\mu$ m and 50 $\mu$ m isotropic voxel size, respectively. The  $\mu$ CT images were binarized by setting a threshold at the midpoint of the two modes. The  $\mu$ MRI images were binarized and registered to the  $\mu$ CT images using the algorithm described in [4] as illustrated in Figure 1. Segmentation of grayscale images generally results in creation of elements disconnected from the main structure. These unconnected parts were removed by a cluster algorithm and matching 3D volumes of  $\mu$ MR and  $\mu$ CT were extracted (three independent subvolumes were extracted from each of the ten images, yielding a total of 30 data sets). The selected subvolumes were converted to voxel-based  $\mu$ FE model and were subjected to six linear  $\mu$ FE analyses to determine the full elastic modulus matrix including three Young's moduli (E11, E22, and E33) and three shear moduli (G23, G31 and G12) using an element-by-element pre-condition conjugate gradient solver.

**Results and Conclusions** Direct comparison of binary TB images from  $\mu$ MRI and  $\mu$ CT is complicated by the apparent thickening of trabeculae in the  $\mu$ MR images caused by the bone-marrow susceptibility discontinuity. The overestimation of bone volume fraction (BVF) can be corrected by moving the histogram peaks approximately to the same location in the gray scale intensity range before segmentation and choosing a constant threshold for all data sets. Figure 2 (a) shows the correlation between BVF derived from  $\mu$ MRI and  $\mu$ CT after histogram correction. Young's and shear moduli, estimated from  $\mu$ MRI were found to be highly correlated, with a slope close to unity, with those derived from  $\mu$ CT (Figures 2b and c). The high correlation between mechanical parameters calculated from  $\mu$ MRI and  $\mu$ CT suggests that the overall trabecular bone network is preserved in  $\mu$ MR images, in spite of lower spatial resolution and locally induced fields from the bone's relative diamagnetism, relative to the gold standard values obtained by  $\mu$ CT.

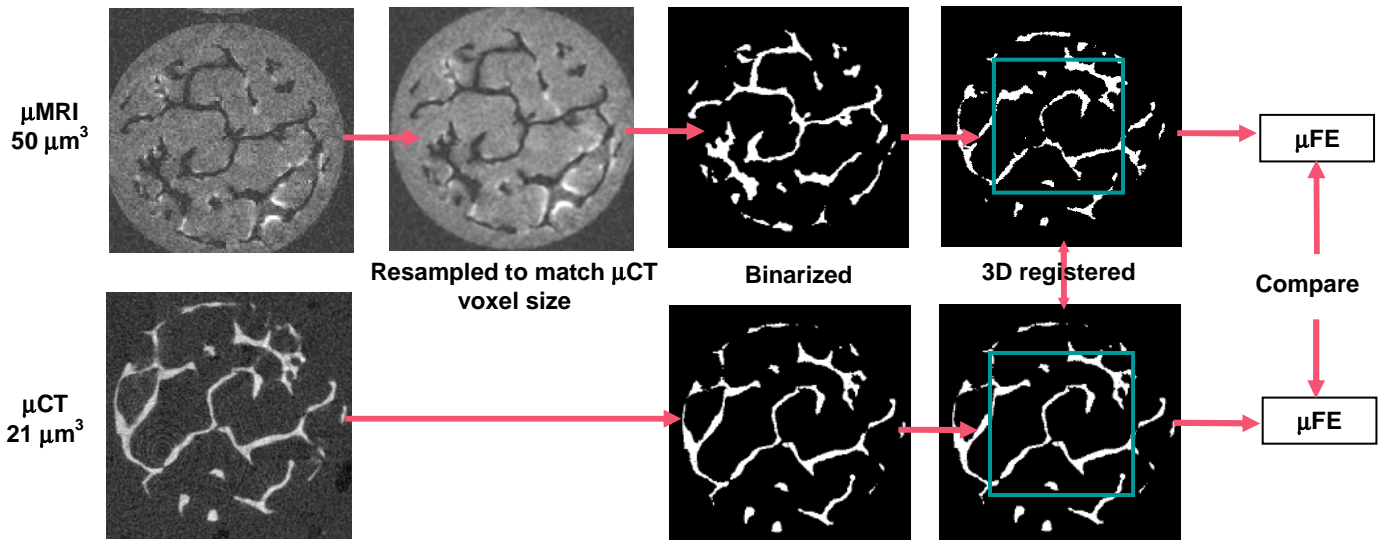
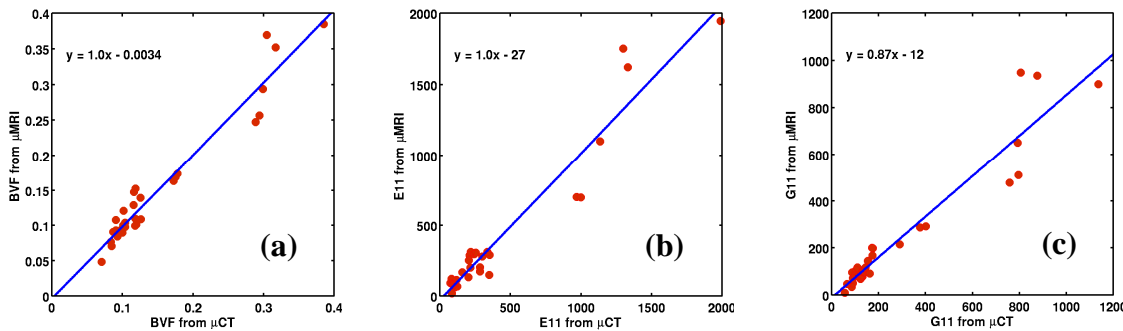


**Figure 1:** Processing steps used to extract TB volume from  $\mu$ MR images that correspond to matching  $\mu$ CT image volumes for  $\mu$ FE analysis. Acquired  $\mu$ MR images were pre-processed, resampled to  $\mu$ CT voxel size and BVF corrected prior to segmentation. Segmented  $\mu$ MR and  $\mu$ CT images were registered and regions of interests were extracted for  $\mu$ FE analysis.



**References**  
 [1] Müller, Harvard Orthop. J, 2002  
 [2] Majumdar, Top. Mag. Reson. Imaging, 2002  
 [3] Wehrli et al., Proc IEEE, 2003  
 [4] Rajapakse et al., SPIE MI, 2008  
 [5] Wehrli et al., NMR in Biomed, 2006

**Figure 2:** Correlation of a) BVF b) Young's modulus and c) shear modulus in the primary direction derived from  $\mu$ MRI and  $\mu$ CT.

**Acknowledgement** NIH R01 AR41443, R01 AR53156 and R01 AR49553.